Dynein light chain rp3 acts as a nuclear matrix-associated transcriptional modulator in a dynein-independent pathway

Ting-Yu Yeh[1], Jen-Zen Chuang[1] and Ching-Hwa Sung[1,2,*]

[1]Department of Ophthalmology and [2]Department of Cell and Development Biology, Weill Medical College of Cornell University, 1300 York Avenue, New York, NY 10021, USA

*Author for correspondence (e-mail: chsung@mail.med.cornell.edu)

Accepted 3 May 2005
Journal of Cell Science 118, 3431-3443 Published by The Company of Biologists 2005
doi:10.1242/jcs.02472

Summary

Cytoplasmic dynein is a motor protein complex involved in microtubule-based cargo movement. Previous biochemical evidence suggests that dynein light chain subunits also exist outside the dynein complex. Here we show that the dynein light chain rp3 is present in both the cytoplasm and the nucleus. Nuclear rp3 binds to and assembles with the transcription factor SATB1 at nuclear matrix-associated structures. Dynein intermediate chain was also detected in the nucleus, but it was dispensable for the rp3-SATB1 interaction. SATB1 facilitates the nuclear localization of rp3, whereas rp3 and dynein motor activity are not essential for nuclear accumulation of SATB1. The nuclear rp3-SATB1 protein complex is assembled with a DNA element of the matrix attachment region of the *Bcl2* gene. Finally, rp3 is involved in SATB1-mediated gene repression of *Bcl2*. Our data provide evidence that dynein subunit rp3 has functions independent of the dynein motor.

Supplementary material available online at
http://jcs.biologists.org/cgi/content/full/118/15/3431/DC1

Key words: Dynein light chain, rp3, SATB1, Nuclear matrix, *Bcl2*

Introduction

Cytoplasmic dynein is the primary candidate for almost all minus-end, microtubule-based motile processes, and hence for an extremely wide range of cellular events. These events include axonal transport, mitotic spindle alignment, nuclear migration, Golgi centrosomal localization and nuclear translocation of transcription factors (Vallee et al., 2004). Each dynein complex consists of two heavy chains (HC; ~530 kDa) that convey ATPase and motor activities plus a group of accessory polypeptides including intermediate chains (IC; ~74 kDa), light intermediate chains (LIC; ~52-61 kDa) and light chains (LC; 8, 14 and 22 kDa) (King et al., 1996a; King et al., 1996b). The IC acts as a scaffolding protein linking the dynactin complex and LC to the HC motor subunit (Mok et al., 2001; Tai et al., 2001). The functions of the remaining subunits are poorly understood, but recent evidence indicates that LCs and LICs can serve as adaptors for cargo recognition and binding (Tai et al., 1999; Young et al., 2000).

One potential mechanism for the regulation of dynein activity is thought to be subunit heterogeneity. There are two genes each for the HC, the IC and the LIC. At least five genes encode different LCs: Tctex-1, rp3, LC8-a, LC8-b and LC7/roadblock (Vallee et al., 2004). The expression of many of the LC isoforms studied so far appears to be highly regulated at the developmental, cellular and subcellular levels (Chuang et al., 2001; Roux et al., 1994; Tai et al., 2001). Nevertheless, little is known about how the subunit assembly is determined and regulated in a given cell. Finally, there are abundant amounts of LC subunits, such as Tctex-1 and LC8, which are not part of a dynein complex (King et al., 1996a; Li et al., 2004; Tai et al., 1998). The existence of dynein-free LC may represent a pool of subunits awaiting assembly into the dynein complex. Alternatively, the LC subunits may function in a dynein-independent pathway. Interestingly, the cytoplasmic dynein LC8 subunit was found to be a subunit of myosin V (Benashski et al., 1997; Espindola et al., 2000), a subunit of flagellar radial spokes (Yang et al., 2001), and was also present in *Arabidopsis*, which has no cytoplasmic dynein (Lawrence et al., 2001). These observations indicated the LC8 may exhibit roles independent of its function in cytoplasmic dynein. Many polypeptides have been identified that interact with the LC subunits Tctex-1 and LC8 (Vallee et al., 2004). Although the ability of Tctex-1 in docking cargoes onto cytoplasmic dynein and hence microtubules has been confirmed (Tai et al., 1999; Tai et al., 2001), it is currently unknown how many of these interaction partners represent true cytoplasmic dynein cargoes. It is equally unclear whether all of these interactions and the cellular activities mediated by such interactions are dynein-dependent.

In interphase cells, eukaryotic chromosomes form topologically constrained loops every 5-200 kb. The loops are organized by anchoring matrix attachment regions (MARs), which are specific DNA sequences at the base of DNA loops, to the nuclear matrix (Cockerill and Garrard, 1986; Mirkovitch et al., 1987). A growing body of evidence suggests that the proteins or protein complexes associated with the nuclear matrix near MAR binding sites are involved in the regulation of replication, transcription, RNA processing and DNA

Journal of Cell Science

Journal of Cell Science

recombination/repair (Boulikas, 1995). For example, the nuclear matrix-associated protein SATB1 binds to a special AT-rich MAR and modulates nucleosome organization and gene expression (de Belle et al., 1998; Goebel et al., 2002; Yasui et al., 2002). Unlike classic transcription factors, which bind individual target genes, SATB1 binds to multiple MAR sites on chromosomes and regulates gene expression globally, primarily as a transcription repressor. For example, thymocytes from SATB1 null mice displayed a large number of gene dysregulation events, which were mostly derepressions (Alvarez et al., 2000).

The present report studies rp3, another LC subunit that shares 55% amino acid identity with Tctex-1. Besides the competition of rp3 with Tctex-1 for binding to IC (Tai et al., 2001), very little is known about the cellular roles of rp3. Using an isoform-specific anti-rp3 antibody that does not crossreact with Tctex-1 (Chuang et al., 2001), we first revealed the nuclear matrix localization of rp3. Subsequent two-hybrid screening identified SATB1 as an rp3 interacting partner. Although rp3 and dynein activity are not essential for the nuclear transport of SATB1, SATB1 assists in the recruitment of nuclear rp3. The rp3 LC subunit is assembled within the protein-DNA complexes formed between the SATB1 and the MAR region of the *Bcl2* gene, and modulates SATB1-mediated gene repression.

Materials and Methods

Antibodies, plasmids and siRNA

Unless otherwise specified, chemicals and tissue culture reagents were purchased from Sigma (St Louis, MO) and Invitrogen (San Francisco, CA), respectively. SATB1 and $p150^{Glued}$ monoclonal antibodies (mAbs) were purchased from BD Biosciences (Hercules, CA); GST and Flag rabbit antibodies and Flag, γ-adaptin, β-tubulin and HC mAbs were from Sigma. C/EBP, SC35 and PML mAbs were from Santa Cruz Biotechnology (Santa Cruz, CA); IC mAb was from Chemicon (Temecula, CA); α-tubulin mAb was from Amersham (Piscataway, NJ); rabbit anti-GFP and Alexa-conjugated secondary antibodies were from Molecular Probes (Eugene, OR). Affinity-purified rabbit anti-rp3 antibody has been described (Chuang et al., 2001).

The plasmids encoding GST, GST-Tctex-1 and GST-rp3 (Tai et al., 1998), and eukaryotic expression vectors encoding Flag-rp3 and rp3 are described elsewhere (Tai et al., 2001). Full-length human rp3 cDNA was fused in-frame downstream to the Gal4DB domain in pPC97, and the resulting plasmid was used as bait for yeast two-hybrid screening. GFP-rp3 fusion construct was generated by inserting the rp3 open reading frame into the N-terminus of GFP in pEGFP-N1 (Clontech Laboratories)

Human SATB1 was RT-PCR amplified from RNA from the human Jurkat cell line using RNeasy (Qiagen, Valencia, CA) and specific primers (forward, 5′-GGAATTCGTATGGATCATTTGAACGAGG-CAACTC-3′; reverse, 5′-GCTCTAGAGTAAATACCAGTGGCACT-GTTGAACG-3′). The PCR fragments were digested with *Eco*RI/*Xba*I and ligated into Flag-pRK5 (Chuang et al., 2001). To generate Flag-STAB1-N, the *Eco*RI/*Bgl*II fragment of Flag-SATB1 was transferred into pBS-KS (Stratagene, La Jolla, CA) to generate an intermediate construct. The *Eco*RI/*Sal*I fragment of the intermediate construct was subsequently transferred back to the Flag-pRK5 to yield Flag-SATB1-N. The DNA fragment for SATB1-C was PCR amplified from Flag-SATB1 (forward, 5′-GGGGATCCCTTTGGAGCAACAGG-3′, and reverse, 5′-GCTCTAGAGTAAATACCAGTGGCACTGTTGAACG-3′), digested with *Bam*HI/*Xba*I, and subcloned into Flag-pRK5 to yield the Flag-SATB1-C expression vector. The PDZ domain of SATB1 was PCR amplified using primers (5′-CGGGATCCATT-GCAAGGAGGAGCATGC-3′ and 5′-GCTCTAGATCACAATGAA-CTCTGATTC-3′), digested with *Bam*HI/*Xba*I, and inserted into Flag-pRK5. Gal4DB-SATB1 was constructed by in-frame insertion of *Bam*I/*Xba*I-cut Flag-SATB1 into pGal4DB.

For tetracycline-regulated Flag-SATB1, the EGFP coding sequence in the vector pBI-EGFP was replaced by the coding sequence for FLAG-SATB1 using the *Eag*I/*Sal*I fragment of Flag-SATB1. The resulting plasmid had the Flag-SATB1 sequence downstream of a minimal CMV promoter under the control of a tetracycline-responsive element.

To generate the *Bcl2* MAR-luciferase reporter construct, the 400-bp *Bcl2* MAR region was PCR amplified from human genomic DNA (5′-gcggatccagcagattcaaatctatggtggtttg-3′. 5′-cggaattctaaagcagcttgg-aggatcttacc-3′). The *Bam*HI/*Eco*RI-digested PCR fragment was subcloned into pBS-KS for an intermediate construct, from which the *Sac*I/*Xho*I fragment was transferred into luciferase reporter pGL2-control vector (Promega). The resulting construct, *Bcl2*-MAR-luc, contains *Bcl2* MAR immediately upstream of the SV40 promoter of pGL2-control.

pTet-off (Clontech), pTK-RL (Promega), pGL2-5Gal4, pSG-VP16, and pGal4DB (Zhou and Chiang, 2001; Sadowski et al., 1988) were gifts of Cheng-Ming Chiang (Case Western Reserve University, Cleveland, OH). Plasmids GFP-IC (gift of Dr Trina Schroer, Johns Hopkins University, Baltimore, MD), myc-p50 dynamintin (gift of Richard Vallee, Columbia University, New York, NY), and pC/EBPβ (gift of Yu-May Lee, Academia Sinica, Taiwan) were also used.

rp3-siRNA (5′-AGAGUGUGUAGAUGGGGUUdTdT-3′ and 5′-AACCCCAUCUACACACUCUdTdT-3′) and the control siRNA (5′-GAGGCUAUAGAAAGCGCAAdTdT-3′ and 5′-UUGCGCUU-UCUAUAGCCUCdTdT-3′) were synthesized by Dharmacon Research. Annealing of each siRNA pair was carried out according to the manufacturer's protocol.

Transient transfection of HEK and HeLa cells was carried out with calcium phosphate or Lipofectamine 2000. In some experiments, siRNA (133 nM final concentration) was co-transfected with plasmids using Lipofectamine 2000. In the Tet-off expression experiments, doxycycline (1 μg/ml) was used to suppress gene expression.

Two-hybrid screening

Using full-length human rp3 in pPC97 as bait, two-hybrid library screening was carried out using a rat brain cDNA library in pPC86 (gift of A. Lanahan, Johns Hopkins University, Baltimore, MD) in yeast strain Y190, as previously described (Tai et al., 1999). Unlike the yeast cells harboring rp3 in the bait plasmid used in the pLexA two-hybrid system that exhibited β-galactosidase activity (i.e. auto-activation) (Douglas et al., 2004), yeasts harboring rp3 in pPC97 bait plasmid were not auto-active in the X-gal filter assays and failed to grow in 3-amino-1,2,4-triazole$^+$/Trp$^-$/Leu$^-$/His$^-$ cultures. Plasmid DNAs isolated from the His$^+$/LacZ$^+$ yeast transformants were retransformed into DH10B and autosequenced. A total of ~1×10^6 recombinants were screened. In addition to SATB1 described in this paper, rp3 itself, which homodimerizes, and IC, which binds to rp3 (Tai et al., 2001), were also repeatedly isolated, validating the two-hybrid screening procedure.

Immunocytochemistry, immunoblotting, immunoprecipitation and pull-down assays

Three different procedures were used to prepare cells for immunolabeling: (1) ice-cold methanol fixation for 5 minutes; (2) 4% paraformaldehyde fixation for 10 minutes followed by 0.1% Triton X-100 treatment for 10 minutes; (3) nuclear matrix preparation essentially as described (Nickerson et al., 1997). Briefly, cells were extracted with ice-cold 0.2% Triton X-100 in CSK buffer (10 mM PIPES, pH 6.8, 300 mM sucrose, 100 mM NaCl, 3 mM $MgCl_2$, 1 mM

Journal of Cell Science

EGTA, 20 mM vanadyl riboside and 1 mM PMSF) for 2 minutes followed by fixation in 4% paraformaldehyde for 40 minutes at 4°C. Cells were then digested in 400 μg/ml DNaseI for 50 minutes at 32°C. All immunolabeled samples were analyzed by Leica TCS SP2 spectral confocal system (Nussloch, Germany).

Pull-down assays were performed as previously described (Tai et al., 1999) with minor modifications. Briefly, ^{35}S-labeled Flag-SATB1 was synthesized in vitro using the TnT-coupled transcription/translation system (Promega, Madison, WI), purified by MicroSpin G-25 spin columns (Amersham), and incubated with glutathione-Sepharose beads (Amersham), which held equal amounts of GST, GST-Tctex-1 and GST-rp3 fusion proteins (Tai et al., 2001). After extensive washing, proteins were eluted by reduced glutathione and used for SDS-PAGE analysis and autoradiography. Both immunoprecipitation and immunoblotting assays were carried out as described (Tai et al., 1998).

Cell fractionation and velocity density gradient sedimentation

The cytosolic and nuclear extracts of cell cultures and dissected brain regions were prepared essentially according to described methods (Hewetson and Chilton, 2003; Hsueh and Lai, 1995; Guerrini et al., 1997). Briefly, in experiments not involving gradient fractionations, cells were harvested in hypotonic buffer (10 mM HEPES, pH 7.9, 1.5 mM $MgCl_2$, 10 mM KCl and 1 mM DTT, 1 mM PMSF, 1 mM EDTA and protease inhibitors) on ice for 5 minutes, homogenized with a Dounce homogenizer (10 strokes with pestle A; 20 strokes with pestle B), and followed by centrifugation at 326 ***g*** for 5 minutes. These supernatants were considered as 'cytosol extracts'. Nuclear proteins were then extracted with nuclear extract buffer (20 mM HEPES pH 7.9, 1.5 mM $MgCl_2$, 0.3 M KCl, 1 mM EDTA, 1 mM DTT, 1 mM PMSF and protease inhibitors) for 30 minutes. After centrifugation (13,800 ***g*** for 15 minutes), the resulting supernatants were considered as 'nuclear extracts'.

In experiments involving sedimentation analysis, cytosolic and nuclear extracts were prepared by following exactly the same procedures described above, except that the microtubule stabilization buffer PEM (80 mM PIPES, pH 6.8, 1 mM EGTA, 1 mM $MgSO_4$, 0.5 mM DTT, 1 mM PMSF and protease inhibitor) was used to replace the hypotonic buffer during the cell harvest. In addition, both cytosol and nuclear extracts were centrifuged further (100,000 ***g*** for 1 hour) prior to their separation on 5-20% linear sucrose gradients as described (Tai et al., 2001).

Electrophoretic mobility shift assay (EMSA)

EMSAs were performed essentially as described (Ramakrishnan et al., 2000) using 10 μg nuclear extracts and ^{32}P-labeled, *Bcl2* MAR oligonucleotide (5′-GATTCTAATTTTTAAGCAAAATATTATTTT-ATG-3′). Antibodies (3 μg) were added to the reaction mixtures for supershift experiments. All samples were separated on 6% polyacrylamide gels.

Luciferase reporter assay

For each transfection, firefly luciferase reporter plasmid pGL2-5Gal4 (1 μg), *Renilla* luciferase reporter plasmid pTK-RL (0.05 μg) and a mixture of pGal4-SATB1 and pcDNA3.1 (0.5 μg) were transfected. In the reporter assays involving *Bcl2*, *Bcl2*-MAR-luc (1 μg) was co-transfected with pTK-RL (0.05 μg) and a combination of expression vectors for SATB1 and/or rp3 (0.4 μg). The pRK5 empty vector was added in some experiments to maintain constant plasmid input. For siRNA experiments, 133.3 nM rp3 siRNA (or control siRNA) was co-transfected with pGL2-5Gal, pTK-RL and pGal4DB-SATB1 described above using Lipofectamine 2000. The relative luciferase activity was calculated based on the amount of luminescence produced by *Renilla* luciferase for each reaction. Transfected cells were harvested 48 hours post transfection, and the dual luciferase reporter assay carried out following the manufacturer's instructions (Promega). More than three independent experiments were performed and the Student's *t*-test was used for statistical analysis.

Quantitative real-time PCR

Total RNA was isolated from the 24-hour transfected HEK cells using RNeasy (Qiagen). RNA (5 μg) was reverse-transcribed using oligo(dT)$_{15}$ primer and SuperScript reverse transcriptase II (Invitrogen). Quantitative real-time PCR was performed in a 15 μl reaction mixture containing 7.5 μl of SYBR^{TM} Green PCR master mix (ABI), 0.5 μl RT products and 100 nM primers using the ABI Prism 7000 Sequence detection system. The primers identified *Bcl2* (sense, 5′-TCCCTCGCTGCACAAATACTC-3′; anti-sense, 5′-AGACGACC-CGATGGCCA-3′) and *GAPDH* (sense, 5′-GGAGTCCCTGCCAC-ACTCAG-3′; anti-sense, 5′-GGTCTACATGGCAACTGTGAGG-3′). Dissociation curves and gel electrophoresis were used to confirm the purity and size of PCR products. The cycle threshold (*Ct*) values of *GAPDH* served as internal controls. The relative transcript levels of *Bcl2* were calculated as $x=2^{-\Delta Ct}$, where $\Delta Ct=Ct_{\text{Bcl2 sample}}-Ct_{\text{Bcl2 control}}$.

Results

rp3 is present in the nucleus

To unravel the biological function of rp3, we first determined its subcellular localization in cultured cells. Immunolabeling using an affinity-purified anti-rp3 antibody showed that rp3 was distributed in the centrosome, cytoplasm and nucleus in methanol-fixed interphase HeLa cells (Fig. 1A). The punctate labeling of the cytoplasm and centrosome was consistent with that described for other dynein subunits (Echeverri et al., 1996; Gill et al., 1991; Paschal et al., 1993). In the cytoplasm, rp3 largely colocalized with IC (Fig. 1A, arrows, middle panel) and dynactin subunit p150^{Glued} (data not shown) on microtubule plus-ends. In the nucleus, weak rp3 labeling was distributed throughout the nucleoplasm, but prominent rp3 signals were found on punctate structures (Fig. 1A). The rp3^{+} nuclear punctae varied in size and number depending on the phase of the cell cycle (data not shown), consistent with the heterogeneous nuclear distribution pattern of rp3 seen in interphase cells. Interestingly, intranuclear IC signals were also noted in HeLa cells and the IC labeling occasionally overlapped with the rp3^{+} nuclear punctae (Fig. 1A, arrowheads, right panel). The nuclear labeling of rp3 was specific and absent in samples lacking primary antibodies (see supplementary material Fig. S1). Consistent with previous reports (Pfarr et al., 1990; Roghi and Allan, 1999), no significant intranuclear labeling of HC was observed in these cells (data not shown).

The nuclear distribution of rp3 and IC was confirmed biochemically using immunoblotting assays of proteins extracted from the cytosolic and the nuclear fractions of HeLa and HEK cells (Fig. 1B). In these assays, tubulin was exclusively detected in the cytosolic fraction, whereas rp3 and IC were detected in both the cytosolic and the nuclear fractions. The nuclear accumulation of both rp3 and IC were also found in various dissected brain regions (e.g. cerebral cortex, hippocampus), where rp3 is enriched (Chuang et al., 2001; King et al., 1998), indicating the nuclear distributions of rp3 and IC are probably physiologically relevant.

To further characterize the nature of rp3-associated punctae, we performed colocalization studies using markers that are known to label various nuclear compartments in

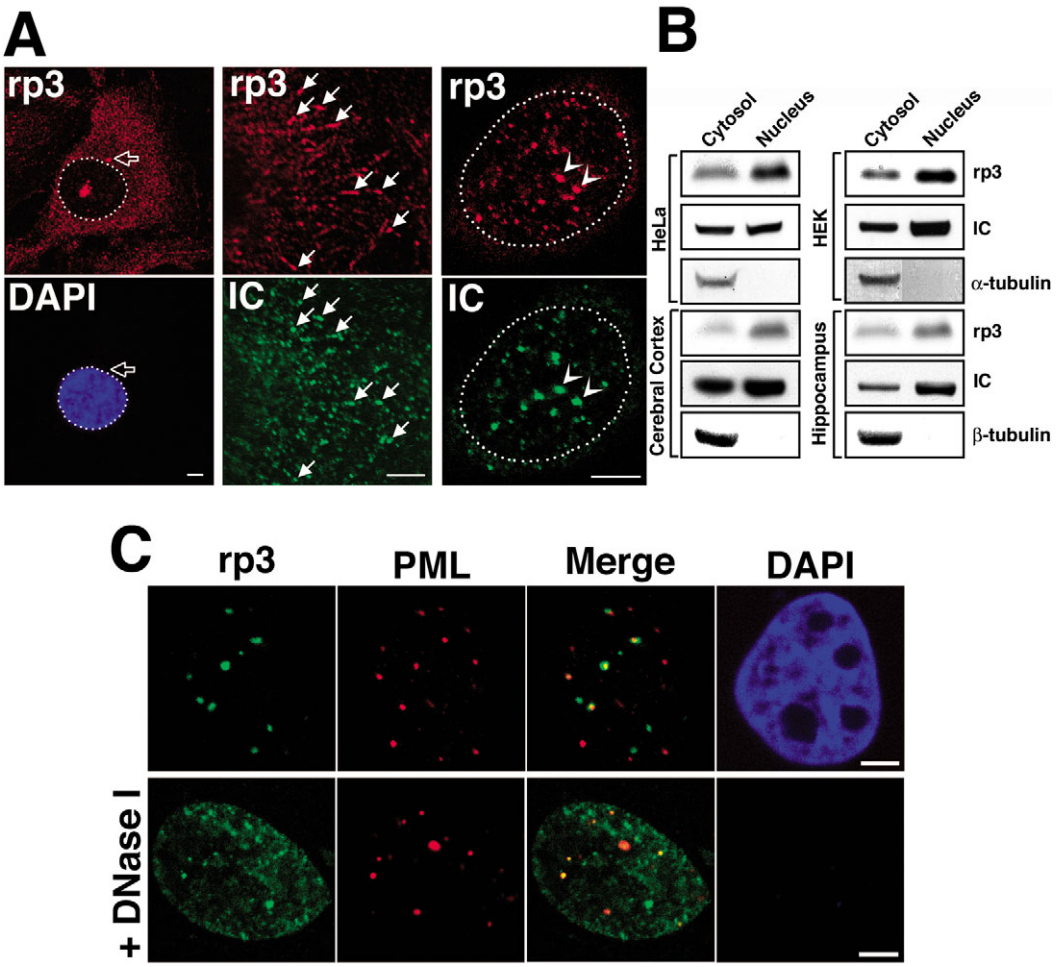

Fig. 1. Subcellular distribution of rp3. (A) Confocal images of HeLa cells double labeled for rp3 and IC. rp3 appears at the centrosome (open arrow, left) and microtubule plus-end, which often colocalized with IC in the cytoplasm (arrows, middle). The focal plane was set so that both cytoplasmic and nuclear signals of rp3 are shown in a single image. In the nucleus, rp3 appears on punctate structures that were occasionally associated with IC labeling (arrowheads, right). Nuclei are circled. (B) Proteins from cytosolic and nuclear fractions of HeLa, HEK and dissected brain regions were analyzed by immunoblotting with the indicated antibodies. (C) Immunolabeling of endogenous rp3 and PML in paraformaldehyde-fixed and Triton X-100-extracted HeLa cells (top panels) or in Triton X-100-extracted, paraformaldehyde-fixed and DNaseI-digested HeLa cells (bottom panels). Lack of DAPI signal in the bottom row indicates complete DNA removal. Bar, 5 μm.

paraformaldehyde-fixed, Triton X-100-extracted HeLa cells. The rp3-labeled nuclear punctae did not co-label with spliceosome marker SC35 (data not shown), indicating they were not nuclear speckles (Fu and Maniatis, 1990). However, the rp3 signals occasionally associated with PML (promyelocytic leukemia protein) nuclear bodies, indicated by PML immunolabeling (Fig. 1C, top row). PML nuclear bodies are structures associated with the nuclear matrix (Ascoli and Maul, 1991; Stuurman et al., 1992). In agreement, PML labeling remained in the nuclear matrix of HeLa cells after chromatin removal by DNase I digestion (Fig. 1C, bottom row). The positive rp3 labeling in the nuclear matrix indicated that some rp3 was also concentrated in nuclear matrix-associated structures.

rp3 interacts with a nuclear matrix-binding transcription factor SATB1

A two-hybrid search for rp3 interacting proteins yielded a cDNA encoding rat SATB1. SATB1 has been reported to be a nuclear matrix-binding transcription factor (de Belle et al., 1998; Dickinson et al., 1992; Nakagomi et al., 1994). Further analysis showed that rp3, but not Tctex-1, was able to interact with SATB1 in the two-hybrid assay (supplementary material Fig. S2). The specificity and the direct interaction between rp3 and SATB1 was also demonstrated in pull-down assays showing that purified GST-rp3, but not the GST or GST-Tctex-1, bound to ^{35}S-labeled, in vitro translated SATB1 (Fig. 2A). The rp3-SATB1 interaction was confirmed by co-immunoprecipitation assays carried out in HEK cells overexpressing Flag-SATB1 and either rp3 or Tctex-1. In these assays, anti-Flag antibody co-immunoprecipitated rp3, but not Tctex-1 (Fig. 2B). The converse experiments showed that anti-rp3, but not anti-Tctex-1 antibody, co-immunoprecipitated SATB1 (data not shown).

Co-immunoprecipitation experiments were then used to map the rp3-binding region of SATB1 in HEK cells transiently transfected with rp3 and Flag-tagged SATB1 fragments (e.g.

Journal of Cell Science

Journal of Cell Science

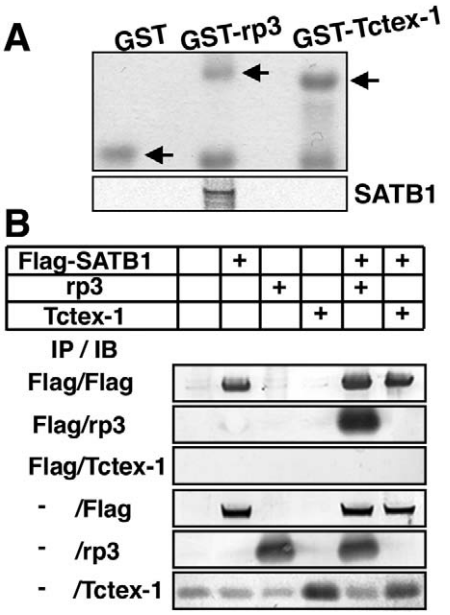

Fig. 2. Interaction between SATB1 and rp3. (A) Recombinant GST, GST-rp3 and GST-Tctex-1 immobilized on glutathione beads were incubated with in vitro-translated, ^{35}S-labeled Flag-SATB1. Eluted proteins were either Coomassie Blue stained (top), or transferred for autoradiography (bottom). Roughly equivalent amounts of GST fusions were used in each experiment (arrows). (B) Anti-Flag antibody immunoprecipitates obtained from HEK cells overexpressing the indicated proteins were immunoblotted with the indicated antibodies (top three rows). The bottom three rows represented the total input used in the immunoprecipitation experiments. Note that a small amount of endogenous Tctex-1 signal was also detected in non-transfected cells using anti-Tctex-1 antibody (bottom row).

SATB1-N, SATB1-C). The SATB1-N fragment (amino acids 1-359) contained the postsynaptic density 95/dlg/ZO-1 homology (PDZ) domain and the SATB1-C fragment (amino acids 360-763) contained the MAR binding region and the atypical homeodomain motif of SATB1 (Fig. 3A) (Galande et al., 2001). Anti-Flag antibody was able to co-immunoprecipitate rp3 from cell lysates that contained either full-length SATB1 or SATB1-N, but not STAB1-C (Fig. 3B). Further experiments showed that Flag-PDZ (amino acids 90-204) was also able to co-immunoprecipitate rp3 (Fig. 3B), indicating that the PDZ domain within the SATB1-N was sufficient for the rp3 interaction.

SATB1 is expressed predominantly in the thymus, but is also found in the brain and several other organs (Alvarez et al., 2000; Dickinson et al., 1992). Using RT-PCR (supplementary material Fig. S3) and immunoblotting assays (supplementary material Fig. S4), we found that SATB1 was expressed in a number of cell lines, including HEK. The biochemical evidence suggested that endogenous SATB1 in HEK cells was, as expected (Cai et al., 2003), primarily nuclear (see Fig. 5A). Similarly, transfected Flag-SATB1 was found to be predominantly intranuclear (Fig. 3A). The SATB1 nuclear labeling had a cage-like, network distribution (data not shown; see Fig. 3D), reminiscent of endogenous SATB1 seen in thymocytes (Cai et al., 2003). The SATB1-N was also nuclear targeted. However, this truncated SATB1 appeared on vacuolar-like structures rather than the network-like structures. These results indicated that the MAR and the homeodomain located on the C-terminal region of SATB1 played critical roles for its proper nuclear subdomain targeting. However, the SATB1-C itself was completely cytoplasmically distributed (Fig. 3A), indicating that a nuclear addressing and/or retention signal was localized at the N-terminal half of SATB1.

SATB1 facilitates the nuclear localization of rp3

To understand the functional relationship between SATB1 and rp3, we examined the distribution of HEK cells ectopically expressing both molecules. In these experiments, cells transfected with GFP-rp3 and a combination of Flag-tagged SATB1 constructs were fixed in paraformaldehyde and extracted in 0.1% Triton X-100 followed by immunolabeling. Confocal analysis showed that the GFP-rp3 signal in singly transfected cells was primarily detected in the cytoplasm (Fig. 3C), even though weak but substantial GFP-rp3 signals were found in the nuclei under less harsh extraction conditions (data not shown). In striking contrast, GFP-rp3 became predominantly concentrated in the nucleus when SATB1 was coexpressed. In the double transfected cells, both rp3 and SATB1 were extensively colocalized in the interchromatin spaces of the nuclei (Fig. 3D, top row) and resistant to the DNase I digestion (Fig. 3D, bottom row), consistent with the notion that these proteins were associated with the nuclear matrix. By contrast, the control GFP co-transfected with SATB1 was completely absent from the nuclear matrix (data not shown), indicating that the nuclear matrix association of GFP-rp3 was not due to the GFP tag.

The SATB1-mediated nuclear localization of rp3 appeared to be very specific as another nuclear transcription factor C/EBPβ had no effect on the subcellular distribution of rp3 (supplementary material Fig. S5). In addition, SATB1 had no effect on the cytosolic distribution of co-transfected GFP-IC fusion protein (Fig. 3C). Similarly, neither the subcellular distribution of GFP nor Tctex-1 was affected by SATB1 (data not shown), further suggesting that the effect of SATB1 on the nuclear localization of rp3 was rather specific. Finally, all these results were reproducible when untagged rp3 or Flag-rp3 was used instead of GFP-rp3 (data not shown).

The above results implied that SATB1 regulated the nuclear localization of rp3 via their protein-protein interaction. Likewise, GFP-rp3 was also predominantly nuclear in cells co-transfected with SATB1-N, and these two molecules were extensively colocalized on the nuclear vacuolar compartments (Fig. 3C). In contrast, the distribution of GFP-rp3 was not affected by the coexpression of SATB1-C. These results verified the location of the rp3-binding domain on SATB1. Additionally, they suggested that the SATB1-rp3 interaction is functional: SATB1 has a regulatory role in the nuclear targeting and/or retention of rp3.

rp3-mediated dynein activity is not critical for SATB1 nuclear transport

It has been shown that dynein-mediated activity is involved in nuclear transport of p53 (Giannakakou et al., 2000). In addition, the rp3 homologue Tctex-1 has a role in cargo recognition and binding (Tai et al., 1999; Tai et al., 2001).

Although the above results suggest that SATB1 regulates subcellular localization of rp3, they did not rule out the converse possibility: rp3 or rp3-mediated dynein activity could also regulate the nuclear transport of SATB1.

Two loss-of-function approaches were taken to test this hypothesis. First, we interfered with dynein activity by overexpressing p50 dynamintin (Echeverri et al., 1996; Roghi and Allan, 1999) and then determined the SATB1 distribution. Our initial experiments showed that the nuclear localization of SATB1 was unchanged when myc-p50 was coexpressed (data not shown). To ensure that dynein activity had been disrupted prior to the SATB1 gene expression, a Tet-off inducible expression system (Gossen and Bujard, 1992) was used. Specifically, HEK cells were transfected with plasmids carrying genes encoding tTA (tetracycline-controlled transactivator; pTet-off), TRE-Flag-SATB1 (Flag-SATB1 ORF is under the control of tetracycline-responsive element) and myc-p50. The transfected cells were cultured in the presence of doxycycline for 24 hours to permit p50 expression while SATB1 expression was under suppression. Cells were subsequently refreshed with doxycycline-free medium, and incubated for an additional 24 hours prior to fixation and immunostaining. As predicted (Roghi and Allan, 1999), overexpressing p50 induced dispersal of Golgi apparatus labeling by γ-adaptin, indicating that dynein activity was impaired (Fig. 4A, bottom panel). However, the nuclear accumulation of SATB1 was unchanged in the cells overexpressing p50 (Fig. 4A, top panel).

A second approach was to silence rp3 expression using RNA interference in conjunction with the Tet-regulated system to

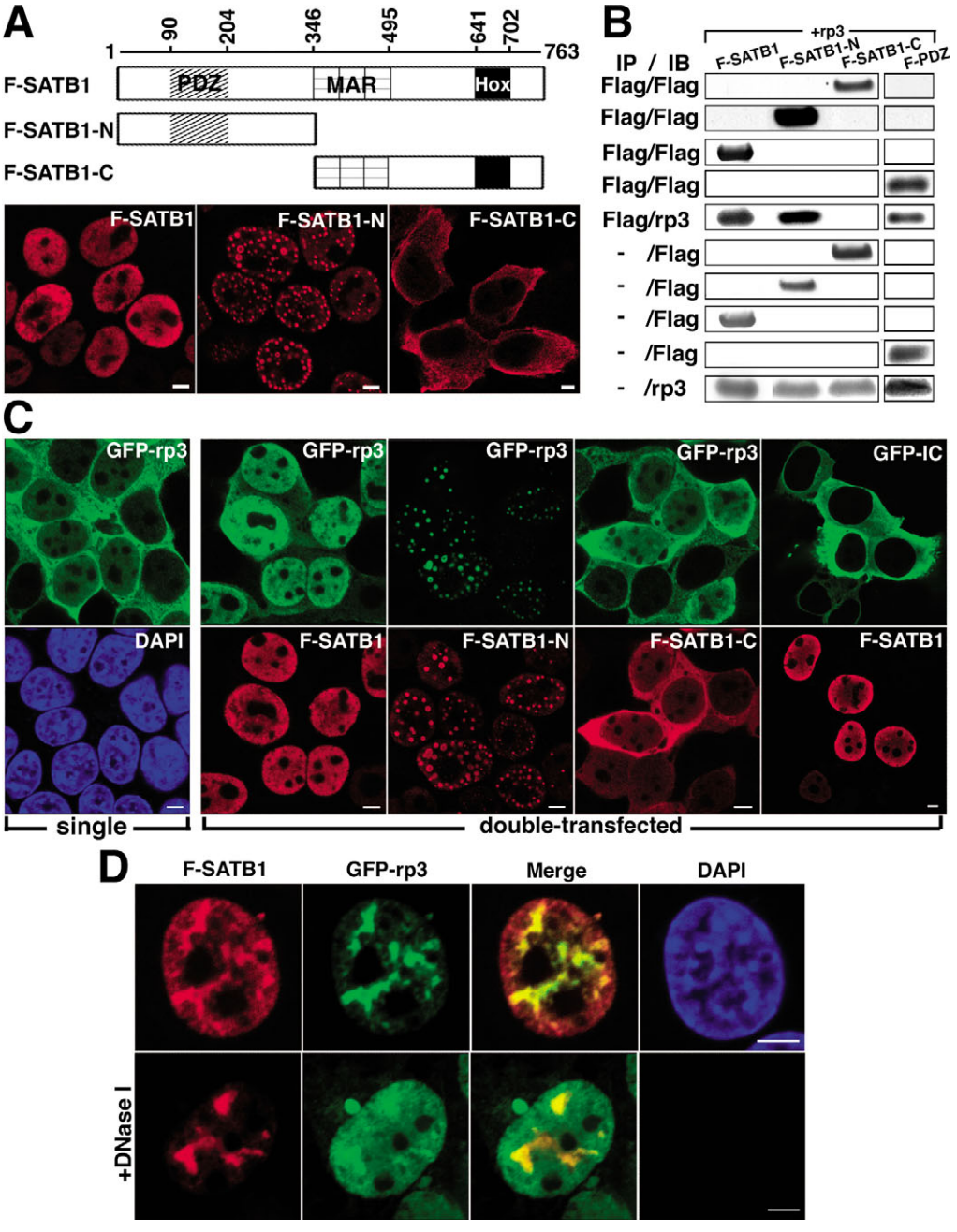

Fig. 3. Nuclear localization of rp3, facilitated by its interaction with the N-terminal region of SATB1. (A) Schematic diagram of SATB1 and the expression constructs of SATB1 used for transfection (top). Boxes label the PDZ domain, the MAR binding domain and the atypical homeodomain (HOX) motif. Immunolabeling of Flag-tagged SATB1, SATB1-N and SATB1-C in transfected HEK cells (bottom). (B) HEK cells co-transfected with rp3 and various Flag-SATB1 constructs were immunoprecipitated with anti-Flag antibody followed by immunoblotting for either Flag or rp3. The immunoblots of total inputs are also shown. (C) Colocalization study of HEKs singly transfected with GFP-rp3, or double transfected with GFP-rp3 or GFP-IC, together with various Flag-SATB1 constructs for GFP (green) and Flag (red). (D) Nuclear Flag-SATB1 (red) and GFP-rp3 (green) were co-distributed in the interchromatin spaces surrounding heterochromatin, the dense regions of DAPI staining, in transfected cells (top panel). Nuclear colocalized Flag-SATB1 and GFP-rp3 remained in the nuclear matrix after DNaseI digestion (bottom panel). Bar, 5 μm.

Journal of Cell Science

delay SATB1 expression. Immunoblotting analysis demonstrated that rp3 siRNA treatment had a strong inhibitory effect on the rp3 expression level (Fig. 4B). Nevertheless, the nuclear SATB1 distribution was the same between the rp3 siRNA-treated and the control siRNA-treated cells (Fig. 4C). Taken together, these results suggested that neither rp3 nor cytoplasmic dynein was critically required for the nuclear transport and/or entry of SATB1.

SATB1 interacts with dynein-free and IC-free rp3

We then sought to delineate the nature of rp3 in the cytosol and in the nucleus and relationship of rp3 to the dynein complex and SATB1. To analyze the endogenous rp3 and SATB1, we preformed velocity density gradient sedimentation using the cytosolic and the nuclear extracts of HEK cells. In the cytosolic fractions, IC and rp3 cosedimented in the ~19S fraction (Fig. 5A, top panel), suggesting that rp3 in the cytoplasm is assembled into dynein complexes (King et al., 2002; Paschal et al., 1987; Schroer and Sheetz, 1991). No SATB1 was detected in any cytosolic fraction.

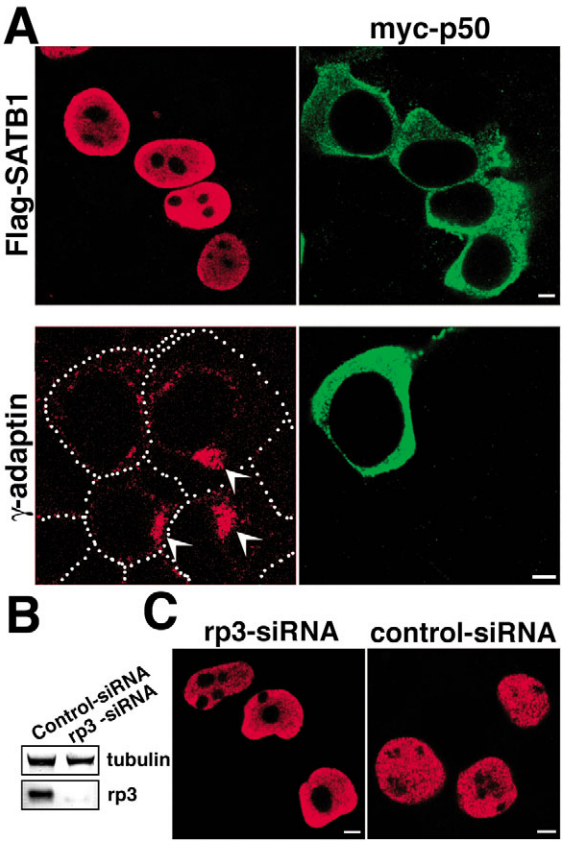

Fig. 4. Nuclear transport of SATB1 and rp3. (A) HEK cells triple transfected with pTet-off, TRE-Flag-SATB1 and myc-p50 were cultured in the presence of doxycycline for 24 hours and switched to regular medium for an additional 24 hours prior to fixation. The fixed cells were double-labeled with anti-Flag and anti-myc (top) or anti-γ-adaptin and anti-myc antibodies (bottom). The centrosomal Golgi distributions in nontransfected cells are indicated (arrowheads). Dotted outlines represent cell margins. (B) Immunoblotting of total cell lysate extracts obtained from cells transfected with either rp3 siRNA or control siRNA and probed with anti-β-tubulin and anti-rp3. (C) HEK cells were triple transfected with pTet-off, TRE-Flag-SATB1, together with either rp3 siRNA or control siRNA. The Flag-SATB1 expression was manipulated as described in A and the cells were immunolabeled with anti-Flag mAb. Bar, 5 μm.

In the nuclear fractions, rp3 sedimented at two peaks corresponding to ~19S and 7-10S (Fig. 5A, middle panel). The rp3 sedimented at ~19S (fractions 4-5), overlapping with the signals of HC and IC and implying that these are probably dynein complexes carried over from the nuclear envelopes and/or cytosol. There is a separate IC-rp3 peak at 7-10S (fractions 9-10). This peak largely overlaps with an SATB1 signal peak in fractions 8-10. To demonstrate that the rp3 and the SATB1 indeed interacted in the lower density fractions, immunoprecipitation using anti-rp3 antibodies of each nuclear fraction confirmed that SATB1 was associated with rp3 in those fractions that were enriched with both rp3 and SATB1 (Fig. 5A, bottom panel). Control experiments using rabbit IgG did not pull down SATB1 from these fractions. Because these experiments were carried out in nontransfected HEK cells, these results strongly supported the notion that the endogenous rp3 and SATB1 interacted with each other in a nuclear protein complex.

The co-fractionation of rp3, IC, and SATB1 and the prior knowledge that rp3 binds directly to IC (Tai et al., 2001) prompted us to examine the relationship between IC and rp3-SATB1 complexes. Immunoprecipitation experiments carried out using (nontransfected) HEK nuclear extracts pulled down endogenous SATB1 along with endogenous rp3 using anti-rp3 antibody (Fig. 5B), but not anti-Tctex-1 antibody (data not shown). Anti-rp3 was also able to co-immunoprecipitate the IC, indicating that either an rp3-IC subcomplex or a protein complex containing rp3 and IC existed in the nuclear extracts. Likewise, the converse experiments showed the IC immunoprecipitates also contained rp3. However, no SATB1 was detected in the IC immunoprecipitates, indicating that SATB1 did not bind to IC or IC-associated rp3.

To further verify that SATB1 only associated with the IC-free form of rp3, sequential immunoprecipitation experiments were carried out. Specifically, a first immunoprecipitation was used to remove IC (and IC-associated complex), and the supernatant was subsequently immunoprecipitated again with either the anti-IC or the anti-rp3 antibodies (Fig. 5C). Consistent with the results above, the first round IC immunoprecipitate contained both IC and rp3, but not SATB1 (Fig. 5C, column 1). IC was not detected in the second round using anti-IC antibody suggesting that IC was completely eliminated during the first procedure (Fig. 5C, column 2). However, rp3 could be isolated from the IC-free nuclear extracts, and the rp3 immunoprecipitates contained SATB1 (Fig. 5C, column 3).

To test the possible SATB1-rp3 interaction in vivo, we showed anti-SATB1 antibody was able to pull down rp3 in the nuclear but not the cytosolic extracts of rat brains (supplementary material Fig. S6). Furthermore, our semi-quantification results suggested that a large proportion, and perhaps the majority, of the free pool of rp3 binds to SATB1 in nuclei of HEK cells and rat brain cells (supplementary material Fig. S7).

rp3 is assembled in SATB1-MAR DNA complexes

We then sought to determine whether rp3 was a component

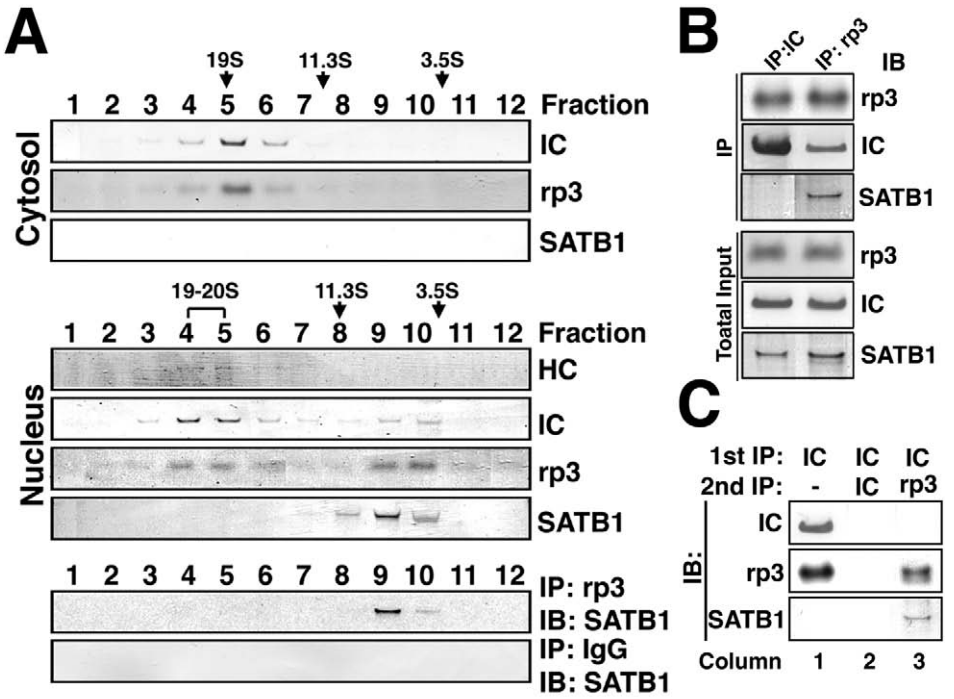

Fig. 5. SATB1 association with rp3 free from dynein complex and IC. (A) Cytosolic and nuclear extracts of HEK cells sedimented in a 5-20% linear sucrose gradient. Fractions were collected, analyzed by SDS-PAGE and immunoblotted with the indicated antibodies. Each nuclear fraction was immunoprecipitated (IP) with anti-rp3 or control rabbit IgG and immunoblotted (IB) with anti-SATB1 antibody (bottom panel). (B) HEK nuclear extracts were immunoprecipitated with either anti-IC or anti-rp3 and immunoblotted with the indicated antibodies. Immunoblots of total inputs are also shown. (C) Nuclear extracts underwent sequential immunoprecipitation procedures. The immunoprecipitates were subjected to immunoblotting with the indicated antibodies. Location of standards for 3.5S, 11.3S and 19S are indicated.

in the complex formed between SATB1 and its target DNA sequences. Of the known SATB1 targeting sequences (Cai et al., 2003; de Belle et al., 1998), we were particularly interested in the 33-bp AT-rich MAR located in the 3′ untranslated region of the *Bcl2* gene (Ramakrishnan et al., 2000). The *Bcl2* MAR is located immediately downstream of the major breakpoint of the translocation site that occurs between *Bcl2* and the IgH locus t(14;18)(q32;q21), a chromosomal rearrangement associated with 85% of follicular small cleaved B cell lymphomas (Yunis et al., 1987). Although SATB1 has been reported to bind *Bcl2* MAR specifically, whether SATB1 regulates *Bcl2* gene expression has not been determined.

We first examined whether rp3 is within the SATB1-*Bcl2* MAR DNA complexes using electrophoretic mobility shift assays (EMSA). In these assays, the radiolabeled *Bcl2* MAR probe was incubated with nuclear extracts of cells overexpressing SATB1, and this reaction gave rise to a number of DNA-protein complexes. Two of these (complex I and II in Fig. 6) were super-shifted by anti-SATB1 to slower-migrating bands (Fig. 6, lane 2), indicating that these two complexes contained SATB1. Consistently, addition of excess unlabeled MAR inhibited the formation of complexes I and II (supplementary material Fig. S8). Control antibodies against Flag, C/EBPβ and GST did not generate any supershift (Fig. 6, lanes 3-5).

EMSA of nuclear extracts obtained from cells double-transfected with SATB1 and Flag-rp3 also had a supershift of the SATB1-containing complex I/II using anti-SATB1 (lane 7). In the same nuclear extract, anti-Flag (Fig. 6, lane 8), but not other control antibodies (lanes 9, 10), also generated a supershift on the complex I/II into a slower migrating complex. These results suggest that rp3 was within the SATB1-*Bcl2* MAR complexes.

Finally, IC was removed from the nuclear extracts of SATB1, Flag-rp3 double transfected cells by immunoprecipitation prior to the EMSA. The complete IC depletion was confirmed by immunoblotting assay (supplementary material Fig. S9). Neither the formation of complex I/II (Fig. 6, lane 11) nor the supershift patterns generated by anti-SATB1- and anti-Flag antibodies (Fig. 6, lane 12, 13) was altered as a result of the absence of IC. Thus, we concluded that the assembly of rp3 into SATB1-*Bcl2* MAR complex was also IC-independent.

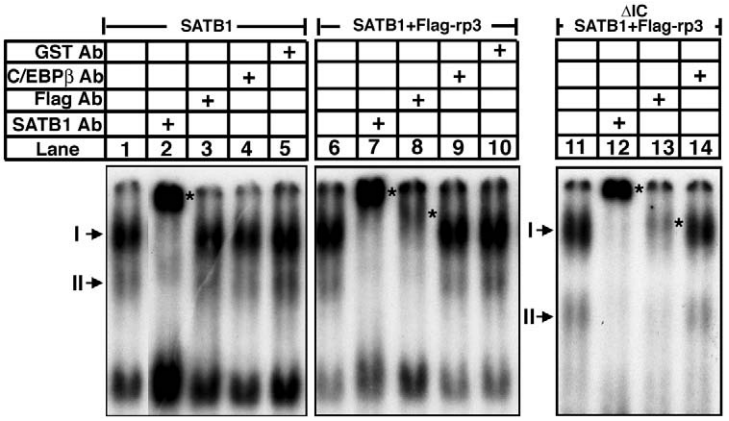

Fig. 6. rp3 assembly within the SATB-1-*Bcl2* MAR DNA complexes. Radiolabeled *Bcl2* MAR was incubated with nuclear extracts of HEK cells transfected with SATB1 (lanes 1-5) or SATB1 together with Flag-rp3 (lanes 6-14). The indicated antibodies were added into each reaction. IC-depleted nuclear extracts were used in lanes 11-14. Arrows indicate the SATB1-containing *Bcl2* MAR complexes (I/II). Asterisks label the slower migrating complexes generated by anti-SATB1 (lanes 2, 7, 12) and anti-Flag antibodies (lanes 8, 13).

Journal of Cell Science

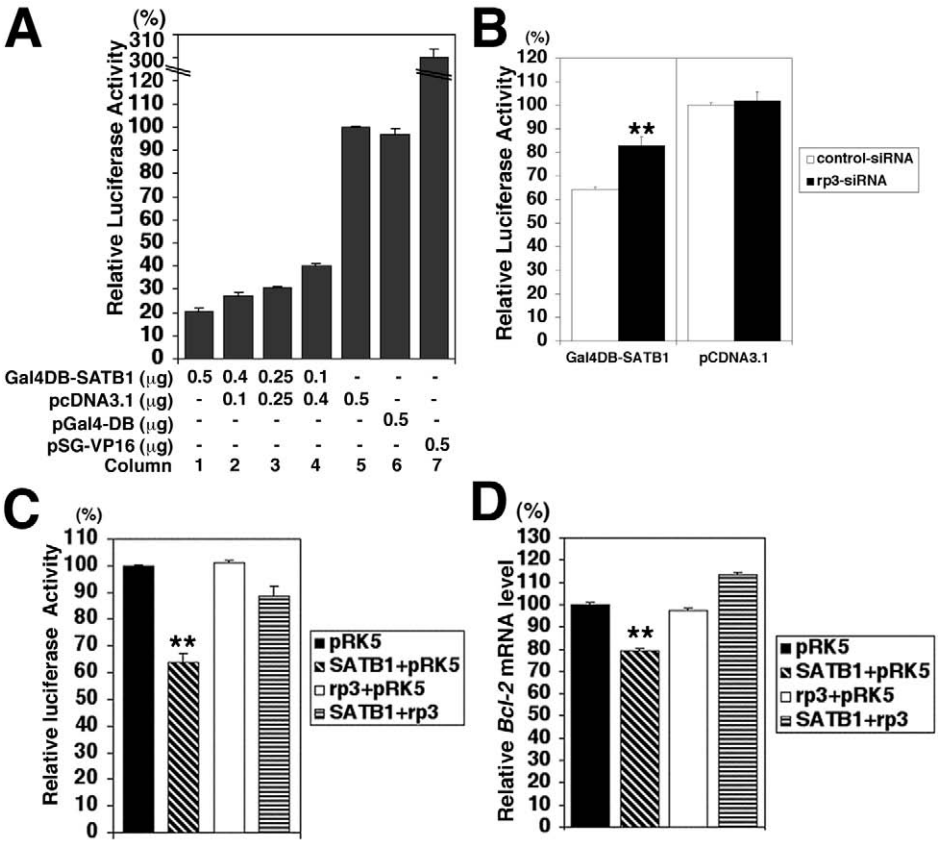

Fig. 7. rp3 involvement in SATB1-mediated transcriptional repression activity and gene regulation of *Bcl2*. (A) HEK cells were transfected with pGL2-5Gal, pTK-RL plus the indicated plasmids. The luciferase activity was measured and that of pcDNA3.1-transfected cells was taken to be 100% (column 5). (B) Luciferase assays of HEK cells transfected with pTK-RL, pGL2-5Gal, pGal4DB-SATB1 and rp3 siRNA or control siRNA. The luciferase activity obtained from cells transfected with pcDNA3.1 and treated with control siRNA was taken to be 100%. (C) rp3 reversed SATB1 suppression effect on *Bcl2*-MAR. Luciferase assays were performed using lysates of HEK cells transfected with pTK-RL, *Bcl2*-MAR-Luc and plasmid combination as indicated. The activity of cells transfected with pRK5 was taken as 100%. (D) *Bcl2* mRNA levels were measured by real-time RT-PCR using RNAs isolated 24 hours after transfection with the indicated plasmids. The *Bcl2* mRNA level of pRK5-transfected cells was taken to be 100%. Significant differences in luciferase activity and mRNA levels were observed (**P<0.01) in indicated cells compared to levels in the control. All values represent the mean±s.e.m. of three separate experiments.

rp3 is a transcriptional modulator of SATB1

We next examined whether rp3 and SATB1 regulate gene transcription. Cells were transfected with constructs expressing a chimera of the Gal4 DNA binding domain fused to SATB1 together with a luciferase reporter pGL2-5Gal, which carries five Gal4 binding sites (Zhou and Chiang, 2001). A dual luciferase reporter system was used measure the reporter activity 48 hours post-transfection. Expression of Gal4DB-SATB1 elicited a dosage-dependent inhibitory effect, up to ~fivefold compared with the pCDNA3.1 empty vector (Fig. 7A, columns 1-5). The negative control Gal4-DB did not affect the luciferase activity (Fig. 7A, column 6) and the positive control Gal4 fusion of VP16 increased the luciferase activity more than threefold (Fig. 7A, column 7). These results were consistent with the notion that SATB1 generally acted as a transcriptional repressor (Liu et al., 1999).

To further investigate rp3 involvement in SATB1-mediated transcriptional regulation, we examined SATB1 repression in cells devoid of rp3. To this end, lysates of HEK cells transfected with pGL2-5Gal reporter, Gal4DB-SATB1 and rp3 siRNA were assayed for luciferase. In controls, the empty vector pcDNA3.1 and control siRNA were used to replace Gal4DB-SATB1 and rp3 siRNA, respectively. Our pilot experiments suggested both the transfection efficiencies and co-transfection efficiency of multiple plasmids were high (>90%); almost no GFP signal can be detected in cells co-transfected with rp3 siRNA and GFP-rp3, even though the GFP signal was not affected by rp3 siRNA in cells co-transfected with GFP alone or GFP-Tctex-1 (data not shown).

Control siRNA and rp3 siRNA did not show a significant difference in luciferase activity of pcDNA3.1-treated cells (Fig. 7B, right panel), These results suggested that rp3 siRNA had little or no effect on the basal level of transcription. By contrast, the rp3 siRNA treatment significantly reversed the Gal4DB-SATB1-mediated luciferase activity repression, suggesting that endogenous rp3 participated in SATB1-mediated gene repression at the transcriptional level. Immunoblotting assays showed that both the cytosolic and nuclear pool of rp3 was significantly reduced in rp3 siRNA-treated cells (data not shown). However, the centrosomal Golgi localization was unaltered in these cells, indicating that the transcriptional regulation effect of rp3 was probably not due to the global dynein function impairment.

We then sought to specifically address how SATB1 and rp3 play a part in MAR-regulated gene expression. To this end, SATB1, rp3 or SATB1/rp3 in combination was co-transfected with a luciferase reporter gene fused to *Bcl2*-MAR element (*Bcl2* MAR-Luc). Compared to the luciferase activity obtained from control cells transfected with empty vector pRK5, SATB1 overexpression significantly suppressed *Bcl2*-MAR-mediated gene transcription (Fig. 7C). Although reproducible, the relatively weak inhibitory effect of SATB1 on gene suppression is similar to that observed in studies of other nuclear matrix binding transcription factors using a similar reporter assay (Liu et al., 1999). By contrast, rp3 itself had little or no effect on *Bcl2*-MAR mediated luciferase activity. Finally, coexpression of rp3 reversed the repressor effect of SATB1 in SATB1/rp3 transfected cells. These results confirmed that the binding of SATB1 to *Bcl2*-MAR was functional and was involved in transcriptional repression. Excess rp3 in transiently transfected

Journal of Cell Science

cells may sequester SATB1 and hence, diminish SATB1-mediated gene suppression.

Finally, we asked whether *Bcl2* is a target gene regulated by SATB1 and rp3. We examined how the endogenous *Bcl2* message level was altered by overexpressed SATB1 and rp3 using quantitative, real-time RT-PCR analysis. Compared to empty vector transfected cells, SATB1 overexpression yielded ~21% reduction in *Bcl2* mRNA levels. Coexpression of rp3 reversed the Bcl2-mediated suppression back to a level higher than that of control cells, even though rp3 alone had little or no effect on *Bcl2* mRNA levels. The relatively weak effect of SATB1 on *Bcl2* gene suppression was consistent with the features shared by many other MAR-binding transcription factors (e.g. CDP, nucleolin) (Liu et al., 1999; Yang et al., 1994). These results together suggested that SATB1 had a repressor role on *Bcl2* gene expression, and rp3 is involved in the SATB1-mediated *Bcl2* gene regulation.

Discussion

In the studies reported here, we demonstrated that rp3, previously recognized as a dynein LC, can function independently of the dynein motor complex as a transcriptional modulator. Both yeast two-hybrid and biochemical evidence suggested that rp3 is associated with nuclear matrix binding transcription factor SATB1. The physiological relevance of the rp3-SATB1 interaction has been demonstrated in two aspects. First, SATB1 positively regulates the nuclear accumulation of rp3. Second, rp3 binds to the MAR at the 3′ untranslated region of the *Bcl2* gene in a SATB1-containing complex, and participates in the SATB1-mediated gene suppression. The present report reveals not only a novel role of rp3 in gene expression regulation, but also an important role of SATB1 in recruiting its own co-factor rp3 for the cooperative gene regulation. Finally, this paper also proposes a novel mechanism for regulation of the *Bcl2* gene.

Subcellular distribution of rp3

Cytoplasmic dynein is known to be present throughout the cytoplasm on microtubule-associated punctae and centrosomes in interphase cells. Dynein also appears on nuclear envelopes and kinetochores during prometaphase and on spindles during metaphase and anaphase (Busson et al., 1998; Pfarr et al., 1990; Steuer et al., 1990). Dynein subunits are also enriched at specific cellular organelles (e.g. Golgi, lysosomes) and/or compartments (e.g. cilia, adhering junction) (Vallee et al., 2004). Here we present immunocytochemical, biochemical and function evidence consistently demonstrating the nuclear expression of rp3.

Regardless of fixation methods (e.g. methanol, paraformaldehyde), immunocytochemistry results consistently reveal intranuclear rp3 signals in various cell lines. Furthermore, the nuclear targeting of ectopically expressed either untagged, Flag-tagged rp3 (data not shown) or GFP-tagged rp3 corroborated the immunostaining results. Immunolabeling of rp3 was most prominent on nuclear matrix-associated structures. Based on morphological characteristics, $rp3^+$ nuclear punctae in HeLa cells are distinct from nuclear speckles, Cajal bodies and Gemini of coiled bodies (Dundr et al., 2004; Liu and Dreyfuss, 1996). However, a subpopulation of $rp3^+$ nuclear punctate labeling partially overlapped with PML nuclear bodies. PML nuclear bodies are subnuclear domains that have been linked to oncogenesis and viral infection (Slack and Gallagher, 1999). In addition, PML bodies could represent potential reservoirs for the biogenesis and/or the storage of nuclear proteins such as transcription factors. In fact, our unpublished results showed that rp3 has also been colocalized with p53, a transcription factor in PML (Pearson and Pelicci, 2001). These are consistent with the nuclear role of rp3 demonstrated in this report. Intriguingly, the nuclear accumulation and distribution patterns of rp3 appear to be tightly regulated. Our unpublished results suggested that the rp3 puncta patterns were at least regulated by the cell cycle and a number of external stimulations, confirming the physiological importance of the nuclear population of rp3.

The presence of rp3 has been previously described in uncharacterized perinuclear structures as well as cytoplasmic punctae in the B104 neuroblastoma cell line (King et al., 1998). The distinct distribution patterns between these two studies are consistent with the diverse subcellular expression patterns of many dynein subunits reported so far. However, we cannot rule out the fact that the distinction was due to the antibody epitope and/or immunostaining procedure.

By immunocytochemistry, Tctex-1 and LC8 signals have also been seen inside the nucleus in interphase cells (Herzig et al., 2000; Kaiser et al., 2003; Tai et al., 1998). Thus many LC subunits may have nuclear functions. In fact, LC8 has been reported to interact with transcription factors NRF-1 and TRPS1 in in vitro assays (Herzig et al., 2000; Kaiser et al., 2003). However, neither the form of the LC8 assembled within dynein nor its target gene was addressed in these cases. It is conceivable that dynein light chains represent a novel class of transcription co-factors.

Our data surprisingly suggested that a subset of IC is also present inside the nucleus. The immunocytochemistry suggested that the IC^+ nuclear puncta are infrequent in methanol-fixed HeLa cells, however, whether the nuclear affiliation of IC is cell cycle dependent has not yet been investigated. The IC signals detected in immunoblots seemed abundant, yet it could be that a fraction of these signals are derived from the dynein complexes associated with nuclear envelopes (Salina et al., 2002). Finally, although the nuclear IC cofractionates with rp3 and interacts with rp3, several lines of evidence coherently suggest that the rp3 associated with SATB1 is free from IC. Finally, the IC is neither critical for the association between rp3 and SATB1 nor the formation of the rp3-SATB1-DNA complexes.

Mechanism of rp3-mediated gene regulation

Higher-order chromatin organization plays an important role in transcriptional regulation. It has been suggested that SATB1 recruits chromatin remodeling complex and histone deacetylase onto specific gene loci to regulate transcription by modifying histone codes and nucleosome positioning (Cai et al., 2003; Yasui et al., 2002). The region of SATB1 that bound to rp3 overlapped with SATB1 binding sites for subunits of chromatin remodeling ACF complex (Yasui et al., 2002) and RNA polymerase II subunit (Durrin and Krontiris, 2002). It is thus possible that rp3 participates in SATB1-mediated chromatin modulation by regulating the recruitment and/or

Journal of Cell Science

Journal of Cell Science

binding of other SATB1-associated proteins. Additionally, structural analysis has suggested that the LC modifies IC subunit conformation upon their association so that the LC-IC protein complex is stabilized (Makokha et al., 2002). It is thus probable that rp3 regulates the assembly of transcription machinery by modulating SATB1 conformation and hence stabilizing the rp3-SATB1 complex or possibly other rp3- or SATB1-associated complexes.

In the present paper, rp3-SATB1 is shown to mediate *Bcl2* gene expression. However, given the relatively large number of SATB1 target genes and its corresponding global effect on gene transcription (Alvarez et al., 2000), it is reasonable to hypothesize that rp3 also participates in most, if not all, SATB1-mediated gene regulation in tissues where these two molecules are both expressed. Finally, rp3 is abundant in brain (Chuang et al., 2001; Roux et al., 1994) and neurological defects were found in SATB1 null mice (Alvarez et al., 2000). Such a coincidence indicates that further studies of the SATB1/rp3 complex may help decipher how nuclear architecture and chromatin structures modulate transcription in the central nervous system.

Dynein light chains and *Bcl2* regulation

The *Bcl2* MAR is located immediately downstream of the major breakpoint of the translocation site that occurs between *Bcl2* and the IgH locus t(14;18)(q32;q21), a chromosomal re-arrangement frequently associated with the follicular B cell lymphomas (Yunis et al., 1987). This translocation relocates the *Bcl2* open reading frame into the *IgH* locus, producing a *Bcl2-IgH* fused transcript and loss of the MAR 3′ untranslated region at der (14). Elevated *Bcl2*-IgH fused mRNA transcription was found in multiple lymphoma cell lines, *Bcl2-IgH* transgenic mice and in many follicular lymphoma patients (McDonnell et al., 1990; Seto et al., 1988). Although the mechanism elevating transcription levels is not fully understood, it has been reported that the *Bcl2* transcription level could be upregulated by the IgH enhancer (Heckman et al., 2003).

Our data raised an interesting possibility that rp3/SATB1-mediated *Bcl2* gene repression may be dysregulated after the t(14;18)(q32;q21) translocation, which may also lead to the abnormally high level of *Bcl2-IgH* mRNA and the pathology of follicular lymphoma. Loss of the negative regulatory element for SATB1 binding in the mouse mammary tumor virus promoter has been suggested to contribute to the elevated mammary tumor viral transcript level and the onset of T-cell lymphoma (Hsu et al., 1988). Finally, the *Myc* oncogene has also been reported to be a target gene of SATB1 (Cai et al., 2003). It would be of interest to examine whether rp3 also participates in SATB1 regulation of *Myc* and other oncogenes.

A recent study suggested that overexpression of LC8 increased the tumorigenic potential of breast cancer cells via a p21-activated kinase-mediated pathway (Vadlamudi et al., 2004). Moreover, LC8 affected cell survival through its interaction with BimL, a *Bcl2* family member, and the LC8-BimL interaction regulated the cell survival function of *Bcl2* in the cytoplasm (Puthalakath et al., 1999). Together with our present data, these results indicate that *Bcl2* may be regulated by dynein light chain subunits at multiple levels, both in the cytoplasm and in the nucleus. Finally, it is conceivable that both LC8 and rp3 participate in oncogenesis albeit through distinct pathways.

Our previous studies showed that the ectopic expression of rp3 reduced the steady-state levels of Tctex-1 (Tai et al., 2001), however, our unpublished results suggest that the attenuation of Tctex-1 level was not controlled at the transcriptional and/or post-transcriptional levels. Whether rp3 can regulate the expression levels of other dynein subunits or its own cargoes through its transcription regulatory role is an open question. Future studies identifying the profiles of gene products regulated by rp3 would be useful in uncovering the physiology of the role of rp3 in gene regulation.

We are indebted to kind gifts from our colleagues. We thank Xiaojing Ma for advice on EMSA and luciferase assays and Lynn Wang for advice on the real-time PCR assay. This work was supported by The Irma T. Hirsch Trust, RPB, The Ruth and Milton Steinbach Fund and NIH grant (EY11307) to C.-H.S.

References

Alvarez, J. D., Yasui, D. H., Niida, H., Joh, T., Loh, D. Y. and Kohwi-Shigematsu, T. (2000). The MAR-binding protein SATB1 orchestrates temporal and spatial expression of multiple genes during T-cell development. *Genes Dev.* **14**, 521-535.

Ascoli, C. A. and Maul, G. G. (1991). Identification of a novel nuclear domain. *J. Cell Biol.* **112**, 785-795.

Benashski, S. E., Harrison, A., Patel-King, R. S. and King, S. M. (1997). Dimerization of the highly conserved light chain shared by dynein and myosin V. *J. Biol. Chem.* **272**, 20929-20935.

Boulikas, T. (1995). Chromatin domains and prediction of MAR sequences. *Int. Rev. Cytol.* **162**, 279-388.

Busson, S., Dujardin, D., Moreau, A., Dompierre, J. and De Mey, J. R. (1998). Dynein and dynactin are localized to astral microtubules and at cortical sites in mitotic epithelial cells. *Curr. Biol.* **8**, 541-544.

Cai, S., Han, H. J. and Kohwi-Shigematsu, T. (2003). Tissue-specific nuclear architecture and gene expression regulated by SATB1. *Nat. Genet.* **34**, 42-51.

Chuang, J. Z., Milner, T. A. and Sung, C. H. (2001). Subunit heterogeneity of cytoplasmic dynein: Differential expression of 14 kDa dynein light chains in rat hippocampus. *J. Neurosci.* **21**, 5501-5512.

Cockerill, P. N. and Garrard, W. T. (1986). Chromosomal loop anchorage of the kappa immunoglobulin gene occurs next to the enhancer in a region containing topoisomerase II sites. *Cell* **44**, 273-282.

de Belle, I., Cai, S. and Kohwi-Shigematsu, T. (1998). The genomic sequences bound to special AT-rich sequence-binding protein 1 (SATB1) in vivo in Jurkat T cells are tightly associated with the nuclear matrix at the bases of the chromatin loops. *J. Cell Biol.* **141**, 335-348.

Dickinson, L. A., Joh, T., Kohwi, Y. and Kohwi-Shigematsu, T. (1992). A tissue-specific MAR/SAR DNA-binding protein with unusual binding site recognition. *Cell* **70**, 631-645.

Douglas, M. W., Diefenbach, R. J., Homa, F. L., Miranda-Saksena, M., Rixon, F. J., Vittone, V., Byth, K. and Cunningham, A. L. (2004). Herpes simplex virus type 1 capsid protein VP26 interacts with dynein light chains RP3 and Tctex1 and plays a role in retrograde cellular transport. *J. Biol. Chem.* **279**, 28522-28530.

Dundr, M., Hebert, M. D., Karpova, T. S., Stanek, D., Xu, H., Shpargel, K. B., Meier, U. T., Neugebauer, K. M., Matera, A. G. and Misteli, T. (2004). In vivo kinetics of Cajal body components. *J. Cell Biol.* **164**, 831-842.

Durrin, L. K. and Krontiris, T. G. (2002). The thymocyte-specific MAR binding protein, SATB1, interacts in vitro with a novel variant of DNA-directed RNA polymerase II, subunit 11. *Genomics* **79**, 809-817.

Echeverri, C. J., Paschal, B. M., Vaughan, K. T. and Vallee, R. B. (1996). Molecular characterization of the 50-kD subunit of dynactin reveals function for the complex in chromosome alignment and spindle organization during mitosis. *J. Cell Biol.* **132**, 617-633.

Espindola, F. S., Suter, D. M., Partata, L. B., Cao, T., Wolenski, J. S., Cheney, R. E., King, S. M. and Mooseker, M. S. (2000). The light chain composition of chicken brain myosin-Va: calmodulin, myosin-II essential

light chains, and 8-kDa dynein light chain/PIN. *Cell Motil. Cytoskel.* **47**, 269-281.

Fu, X. D. and Maniatis, T. (1990). Factor required for mammalian spliceosome assembly is localized to discrete regions in the nucleus. *Nature* **343**, 437-441.

Galande, S., Dickinson, L. A., Mian, I. S., Sikorska, M. and Kohwi-Shigematsu, T. (2001). SATB1 cleavage by caspase 6 disrupts PDZ domain-mediated dimerization, causing detachment from chromatin early in T-cell apoptosis. *Mol. Cell. Biol.* **21**, 5591-5604.

Giannakakou, P., Sackett, D. L., Ward, Y., Webster, K. R., Blagosklonny, M. V. and Fojo, T. (2000). p53 is associated with cellular microtubules and is transported to the nucleus by dynein. *Nat. Cell Biol.* **2**, 709-717.

Gill, S. R., Schroer, T. A., Szilak, I., Steuer, E. R., Sheetz, M. P. and Cleveland, D. W. (1991). Dynactin, a conserved, ubiquitously expressed component of an activator of vesicle motility mediated by cytoplasmic dynein. *J. Cell Biol.* **115**, 1639-1650.

Goebel, P., Montalbano, A., Ayers, N., Kompfner, E., Dickinson, L., Webb, C. F. and Feeney, A. J. (2002). High frequency of matrix attachment regions and cut-like protein x/CCAAT-displacement protein and B cell regulator of IgH transcription binding sites flanking Ig V region genes. *J. Immunol.* **169**, 2477-2487.

Gossen, M. and Bujard, H. (1992). Tight control of gene expression in mammalian cells by tetracycline-responsive promoters. *Proc. Natl. Acad. Sci. USA* **89**, 5547-5551.

Guerrini, L., Molteni, A., Wirth, T., Kistler, B. and Blasi, F. (1997). Glutamate-dependent activation of NF-kappaB during mouse cerebellum development. *J. Neurosci.* **17**, 6057-6063.

Heckman, C. A., Cao, T., Somsouk, L., Duan, H., Mehew, J. W., Zhang, C. Y. and Boxer, L. M. (2003). Critical elements of the immunoglobulin heavy chain gene enhancers for deregulated expression of bcl-2. *Cancer Res.* **63**, 6666-6673.

Herzig, R. P., Andersson, U. and Scarpulla, R. C. (2000). Dynein light chain interacts with NRF-1 and EWG, structurally and functionally related transcription factors from humans and drosophila. *J. Cell Sci.* **113**, 4263-4273.

Hewetson, A. and Chilton, B. S. (2003). An Sp1-NF-Y/progesterone receptor DNA binding-dependent mechanism regulates progesterone-induced transcriptional activation of the rabbit RUSH/SMARCA3 gene. *J. Biol. Chem.* **278**, 40177-40185.

Hsu, C. L., Fabritius, C. and Dudley, J. (1988). Mouse mammary tumor virus proviruses in T-cell lymphomas lack a negative regulatory element in the long terminal repeat. *J. Virol.* **62**, 4644-4652.

Hsueh, Y. P. and Lai, M. Z. (1995). Overexpression of activation transcriptional factor 1 in lymphomas and in activated lymphocytes. *J. Immunol.* **154**, 5675-5683.

Kaiser, F. J., Tavassoli, K., Van den Bemd, G. J., Chang, G. T., Horsthemke, B., Moroy, T. and Ludecke, H. J. (2003). Nuclear interaction of the dynein light chain LC8a with the TRPS1 transcription factor suppresses the transcriptional repression activity of TRPS1. *Hum. Mol. Genet.* **12**, 1349-1358.

King, S. J., Bonilla, M., Rodgers, M. E. and Schroer, T. A. (2002). Subunit organization in cytoplasmic dynein subcomplexes. *Protein Sci.* **11**, 1239-1250.

King, S. M., Barbarese, E., Dillman, J. F. I., Patel-King, R. S., Carson, J. H. and Pfister, K. K. (1996a). Brain cytoplasmic and flagellar outer arm dyneins share a highly conserved Mr 8000 light chain. *J. Biol. Chem.* **271**, 19358-19366.

King, S. M., Dillman, J. F. R., Benashski, S. E., Lye, R. J., Patel-King, R. S. and Pfister, K. K. (1996b). The mouse *t*-complex-encoded protein Tctex-1 is a light chain of brain cytoplasmic dynein. *J. Biol. Chem.* **271**, 32281-32287.

King, S. M., Barbarese, E., Dillman, J. F., 3rd, Benashski, S. E., Do, K. T., Patel-King, R. S. and Pfister, K. K. (1998). Cytoplasmic dynein contains a family of differentially expressed light chains. *Biochemistry* **37**, 15033-15041.

Lawrence, C. J., Morris, N. R., Meagher, R. B. and Dawe, R. K. (2001). Dyneins have run their course in plant lineage. *Traffic* **2**, 362-363.

Li, M. G., Serr, M., Newman, E. A. and Hays, T. S. (2004). The Drosophila tctex-1 light chain is dispensable for essential cytoplasmic dynein functions but is required during spermatid differentiation. *Mol. Biol. Cell* **15**, 3005-3014.

Liu, J., Barnett, A., Neufeld, E. J. and Dudley, J. P. (1999). Homeoproteins CDP and SATB1 interact: potential for tissue-specific regulation. *Mol. Cell. Biol.* **19**, 4918-4926.

Liu, Q. and Dreyfuss, G. (1996). A novel nuclear structure containing the survival of motor neurons protein. *EMBO J.* **15**, 3555-3565.

Makokha, M., Hare, M., Li, M., Hays, T. and Barbar, E. (2002). Interactions of cytoplasmic dynein light chains Tctex-1 and LC8 with the intermediate chain IC74. *Biochemistry* **41**, 4302-4311.

McDonnell, T. J., Nunez, G., Platt, F. M., Hockenberry, D., London, L., McKearn, J. P. and Korsmeyer, S. J. (1990). Deregulated Bcl-2-immunoglobulin transgene expands a resting but responsive immunoglobulin M and D-expressing B-cell population. *Mol. Cell. Biol.* **10**, 1901-1907.

Mirkovitch, J., Gasser, S. M. and Laemmli, U. K. (1987). Relation of chromosome structure and gene expression. *Philos. Trans. R. Soc. Lond. Ser. B* **317**, 563-574.

Mok, Y. K., Lo, K. W. and Zhang, M. (2001). Structure of Tctex-1 and its Interaction with cytoplasmic dynein intermediate chain. *J. Biol. Chem.* **276**, 14067-14074.

Nakagomi, K., Kohwi, Y., Dickinson, L. A. and Kohwi-Shigematsu, T. (1994). A novel DNA-binding motif in the nuclear matrix attachment DNA-binding protein SATB1. *Mol. Cell. Biol.* **14**, 1852-1860.

Nickerson, J. A., Krockmalnic, G., Wan, K. M. and Penman, S. (1997). The nuclear matrix revealed by eluting chromatin from a cross-linked nucleus. *Proc. Natl. Acad. Sci. USA* **94**, 4446-4450.

Paschal, B. M., Shpetner, H. S. and Vallee, R. B. (1987). MAP 1C is a microtubule-activated ATPase which translocates microtubules in vitro and has dynein-like properties. *J. Cell Biol.* **105**, 1273-1282.

Paschal, B. M., Holzbaur, E. L., Pfister, K. K., Clark, S., Meyer, D. I. and Vallee, R. B. (1993). Characterization of a 50-kDa polypeptide in cytoplasmic dynein preparations reveals a complex with p150GLUED and a novel actin. *J. Biol. Chem.* **268**, 15318-15323.

Pearson, M. and Pelicci, P. G. (2001). PML interaction with p53 and its role in apoptosis and replicative senescence. *Oncogene* **20**, 7250-7256.

Pfarr, C. M., Coue, M., Grissom, P. M., Hays, T. S., Porter, M. E. and McIntosh, J. R. (1990). Cytoplasmic dynein is localized to kinetochores during mitosis. *Nature* **345**, 263-265.

Puthalakath, H., Huang, D., O'Reilly, L., King, S. and Strasser, A. (1999). The proapoptotic activity of the Bcl-2 family member Bim is regulated by interaction with the dynein motor complex. *Mol. Cell* **3**, 287-296.

Ramakrishnan, M., Liu, W. M., DiCroce, P. A., Posner, A., Zheng, J., Kohwi-Shigematsu, T. and Krontiris, T. G. (2000). Modulated binding of SATB1, a matrix attachment region protein, to the AT-rich sequence flanking the major breakpoint region of BCL2. *Mol. Cell. Biol.* **20**, 868-877.

Roghi, C. and Allan, V. J. (1999). Dynamic association of cytoplasmic dynein heavy chain 1a with the Golgi apparatus and intermediate compartment. *J. Cell Sci.* **112**, 4673-4685.

Roux, A.-F., Rommens, J., McDowell, C., Anson-Cartwright, L., Bell, S., Schappert, K., Fishman, G. A. and Musarella, M. (1994). Identification of a gene from Xp21 with similarity to the tctex-1 gene of the murine *t* complex. *Hum. Mol. Genet.* **3**, 257-263.

Sadowski, I., Ma, J., Triezenberg, S. and Ptashne, M. (1988). GAL4-VP16 is an unusually potent transcriptional activator. *Nature* **335**, 563-564.

Salina, D., Bodoor, K., Eckley, D. M., Schroer, T. A., Rattner, J. B. and Burke, B. (2002). Cytoplasmic dynein as a facilitator of nuclear envelope breakdown. *Cell* **108**, 97-107.

Schroer, T. A. and Sheetz, M. P. (1991). Two activators of microtubule-based vesicle transport. *J. Cell Biol.* **115**, 1309-1318.

Seto, M., Jaeger, U., Hockett, R. D., Graninger, W., Bennett, S., Goldman, P. and Korsmeyer, S. J. (1988). Alternative promoters and exons, somatic mutation and deregulation of the Bcl-2-Ig fusion gene in lymphoma. *EMBO J.* **7**, 123-131.

Slack, J. L. and Gallagher, R. E. (1999). The molecular biology of acute promyelocytic leukemia. *Cancer Treat. Rev.* **99**, 75-124.

Steuer, E., Wordeman, L., Schroer, T. and Sheetz, M. (1990). Localization of cytoplasmic dynein to mitotic spindles and kinetochores. *Nature* **345**, 266-268.

Stuurman, N., de Graaf, A., Floore, A., Josso, A., Humbel, B., de Jong, L. and van Driel, R. (1992). A monoclonal antibody recognizing nuclear matrix-associated nuclear bodies. *J. Cell Sci.* **101**, 773-784.

Tai, A. W., Chuang, J.-Z. and Sung, C.-H. (1998). Localization of Tctex-1, a cytoplasmic dynein light chain, to the Golgi apparatus and evidence for dynein complex heterogeneity. *J Biol. Chem.* **273**, 19639-19649.

Tai, A. W., Chuang, J.-Z., Bode, C., Wolfrum, U. and Sung, C.-H. (1999). Rhodopsin's carboxy-terminal cytoplasmic tail acts as a membrane receptor for cytoplasmic dynein by binding to the dynein light chain Tctex-1. *Cell* **97**, 877-887.

Tai, A. W., Chuang, J.-Z. and Sung, C.-H. (2001). Cytoplasmic dynein

Journal of Cell Science

regulation by subunit heterogeneity and its role in apical transport. *J. Cell Biol.* **153**, 1499-1509.

Vadlamudi, R. K., Bagheri-Yarmand, R., Yang, Z., Balasenthil, S., Nguyen, D., Sahin, A. A., Den Hollander, P. and Kumar, R. (2004). Dynein light chain **1**, a p21-activated kinase 1-interacting substrate, promotes cancerous phenotypes. *Cancer Cell* **5**, 575-585.

Vallee, R. B., Williams, J. C., Varma, D. and Barnhart, L. E. (2004). Dynein: An ancient motor protein involved in multiple modes of transport. *J. Neurobiol.* **58**, 189-200.

Yang, P., Diener, D. R., Rosenbaum, J. L. and Sale, W. S. (2001). Localization of calmodulin and dynein light chain LC8 in flagellar radial spokes. *J. Cell Biol.* **153**, 1315-1326.

Yang, T. H., Tsai, W. H., Lee, Y. M., Lei, H. Y., Lai, M. Y., Chen, D. S., Yeh, N. H. and Lee, S. C. (1994). Purification and characterization of nucleolin and its identification as a transcription repressor. *Mol. Cell. Biol.* **14**, 6068-6074.

Yasui, D., Miyano, M., Cai, S., Varga-Weisz, P. and Kohwi-Shigematsu, T. (2002). SATB1 targets chromatin remodelling to regulate genes over long distances. *Nature* **419**, 641-645.

Young, A., Dictenberg, J. B., Purohit, A., Tuft, R. and Doxsey, S. J. (2000). Cytoplasmic dynein-mediated assembly of pericentrin and gamma tubulin onto centrosomes. *Mol. Biol. Cell* **11**, 2047-2056.

Yunis, J. J., Frizzera, G., Oken, M. M., McKenna, J., Theologides, A. and Arnesen, M. (1987). Multiple recurrent genomic defects in follicular lymphoma. A possible model for cancer. *New Engl. J. Med.* **316**, 79-84.

Zhou, T. and Chiang, C. M. (2001). The intronless and TATA-less human TAF(II)55 gene contains a functional initiator and a downstream promoter element. *J. Biol. Chem.* **276**, 25503-25511.

Journal of Cell Science